New Journal of Physics
The open access journal at the forefront of physics
Deutsche Physikalische Gesellschaft DPG | IOP Institute of Physics

High fidelity readout of a transmon qubit using a superconducting low-inductance undulatory galvanometer microwave amplifier

Yanbing Liu[1], Srikanth J Srinivasan[1,2], D Hover[3], Shaojiang Zhu[3], R McDermott[3] and A A Houck[1]

[1] Department of Electrical Engineering, Princeton University, Princeton, New Jersey 08544, USA
[2] IBM T. J. Watson Research Center, Yorktown Heights, New York 10598, USA
[3] Department of Physics, University of Wisconsin, Madison, Wisconsin 53706, USA
E-mail: ylfour@princeton.edu

Received 28 April 2014, revised 22 September 2014
Accepted for publication 29 September 2014
Published 4 November 2014

New Journal of Physics **16** (2014) 113008

doi:10.1088/1367-2630/16/11/113008

Abstract

We report high-fidelity, quantum non-demolition, single-shot readout of a superconducting transmon qubit using a dc-biased superconducting low-inductance undulatory galvanometer (SLUG) amplifier. The SLUG improves the system signal-to-noise ratio by 6.5 dB in a 20 MHz window compared with a bare high electron mobility transistor amplifier. An optimal cavity drive pulse is chosen using a genetic search algorithm, leading to a maximum combined readout and preparation fidelity of 91.9% with a measurement time of $T_{\mathrm{meas}} = 200$ ns. Using post-selection to remove preparation errors caused by heating, we realize a combined preparation and readout fidelity of 94.3%.

Keywords: superconducting qubit, microwave amplifier, genetic algorithm

1. Introduction

Scalable fault-tolerant quantum computation with superconducting qubits requires high fidelity measurement. Moreover, having a quantum non-demolition (QND) measurement, in which a qubit remains in its state after measurement, enables or facilitates many quantum information

processing techniques such as state preparation through measurement and error correction. Long coherence times and low noise amplifiers are both essential in resolving a qubit state quickly and with high-fidelity. Several kinds of Josephson parametric amplifiers (JPA) have been shown to operate at or near the quantum limit, and these indeed enabled high fidelity ($> 93\%$) qubit measurement [1–3]. Similarly, microstrip superconducting quantum inference device (SQUID) amplifiers (MSA) [4, 5] have been used to reduce measurement noise in circuit quantum electrodynamics (cQED), but it is still challenging to engineer the MSA so that it has large enough gain and low enough noise at relevant microwave frequencies [6–8].

2. The SLUG amplifier and the transmon qubit

In this manuscript, we rely on a SLUG [9] microwave amplifier to boost the measurement signal-to-noise ratio (SNR). The SLUG is incorporated as a preamplifier preceding the standard high electron mobility transistor (HEMT) amplifier. Unlike parametric amplifiers which require a microwave pump, the SLUG needs only two dc biases for current and flux through its SQUID loop. To sample gigahertz oscillations, the input microwave current is directly injected into the dc-SQUID loop. The resulting oscillatory output voltage serves as an amplified signal. Highly optimized devices are expected to achieve gain greater than 15 dB, bandwidth of several hundred MHz, and added noise of order one quantum in the frequency range of 5–10 GHz [10]. In addition to simpler biasing conditions, the SLUG has a higher saturation power and the potential for directional amplification [11]. In Josephson directional amplifier, directionality is achieved by two stages of parametric conversion combined with wave interference. In the SLUG, the SQUID converts an input signal that is differential with respect to the junction phases to a much larger common-mode output signal; ideally, a common mode signal applied to the output will produce negligible differential signal at the input.

In our measurement system, the SLUG is placed in a μ metal shield and anchored to the base plate of the dilution refrigerator. We have a microwave switch to bypass the SLUG with a through co-axial line, enabling us to calibrate the SNR of the system with and without the SLUG in the measurement chain. The SLUG is characterized by scanning the flux and the current biases and we bias at the point where the gain-bandwidth product is close to its maxinum at the measurement frequency. For the parameters we choose, the SNR improves by 6.5 dB in a 20 MHz window compared with the bare HEMT amplifier, which has a quoted device noise temperature of 4.1 K. The noise performance does not reach the state of the art JPAs as the shunting resistors of the SQUID make the SLUG amplifier intrinsically dissipative. In addition, we find that two isolators, providing 36 dB of isolation, are necessary to protect the sample from amplifier backaction. With only one isolator, the broadband radiation from the SLUG amplifier thermalizes the transmon qubit and greatly shortens its coherence time.

Our cQED system consists of a transmon qubit dispersively coupled to a coplanar waveguide $\lambda/2$ resonator. The system then is well-described by the Jaynes–Cummings model in the linear regime. The measurement exploits the fact that the cavity resonance frequency depends on the state of the qubit [12]. In other words, the qubit information is encoded in the amplitude and phase of microwave transmission through the cavity. The device is mounted in a copper box wrapped with MCS ECCOSORB tape (Emerson and Cuming) to protect it from external radiation and anchored to the 20 mK base temperature stage of a dry dilution refrigerator. Simplified circuit diagram of the measurement setup is shown in figure 1. The

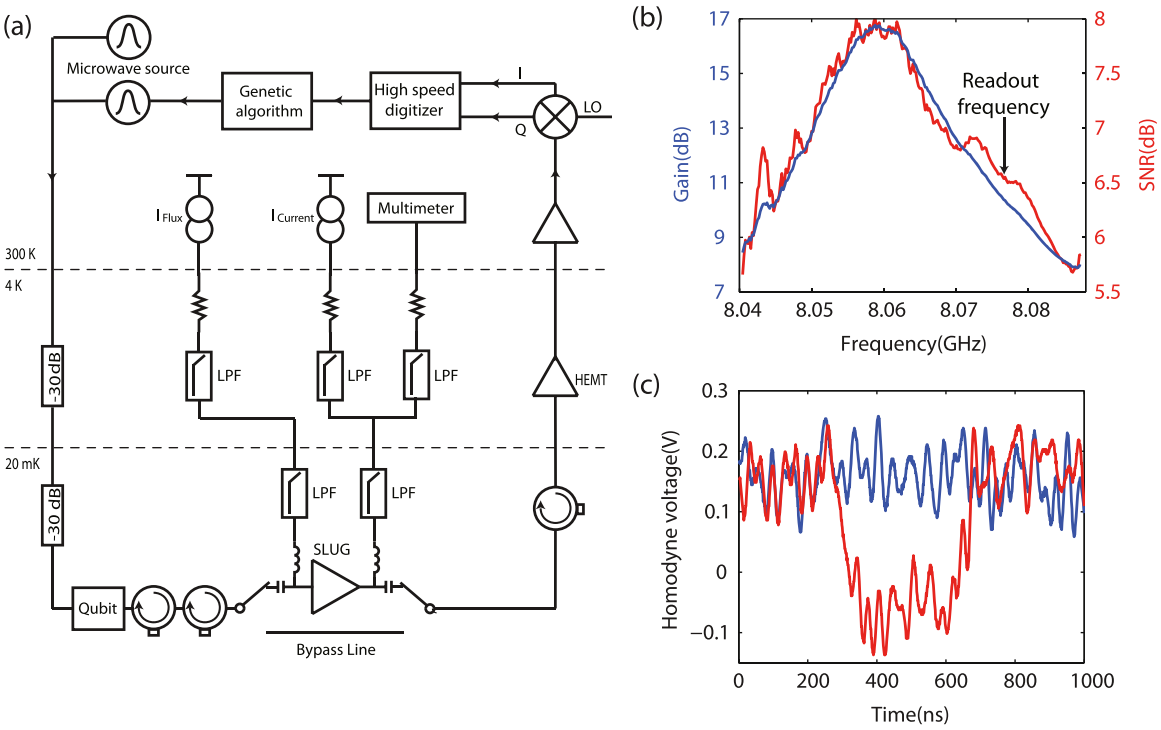

Figure 1. (a) Schematic representation of the measurement setup. Both the device and the SLUG amplifier are placed in μ-metal magnetic shields. The SLUG is dc biased through two bias tee. (b) Gain (red) and SNR improvement (blue) in the bias condition used in this experiment. (c) Quantum jumps could be observed in individual readout traces. Both traces are taken when the qubit is initially in the ground state. The red trace shows the qubit jumps to the exited state and jumps back to the ground state.

parameters of our cQED system are designed to achieve fast and accurate readout of the qubit. Specifically, the cavity leak rate κ has to be high enough to enable fast readout while it has to be not signifigantly larger than the dispersive shift and not effect the lifetime of the qubit (Purcell effect). Moreover, the cavity has to fall well within the bandwidth of the SLUG. Standard spectroscopy techniques are used to measure a cavity resonant frequency and leak rate of $\omega_c/2\pi = 8.081$ GHz and $\kappa/2\pi = 10$ MHz, respectively. The first transition frequency and the anharmonicity of the fixed-frequency transmon qubit are $\omega_q/2\pi = 5.0353$ GHz and $\alpha = 233$ MHz. The qubit-cavity coupling strength is $g/2\pi = 67.6$ MHz which results in a dispersive shift $2\chi/2\pi = 3$ MHz. The relaxation time of the qubit is $T_1 = 2.8\,\mu$s, while the Ramsey decay time is $T_2^* = 2\,\mu$s.

3. High fidelity single-shot readout and genetic algorithm

The improved SNR results in substantial improvement in the qubit readout. The qubit is passively initialized in the ground state and driven to the excited state with a 40 ns Gaussian-envelope π pulse (the pulse is truncated to $\pm 4\sigma$ from the center). After preparation, the qubit state is measured with a 2 μs pulse at a frequency close to the cavity resonance. We optimize fidelity empirically by varying measurement parameters including the pulse frequency, the

pulse power and the pulse shape. The fidelity is calculated with an optimal boxcar filter [17] using 40 000 ground and excited state preparations for each set of system parameters.

Using a square measurement pulse, we first optimize the power and frequency of the readout pulse in the linear regime [13]. Increasing power increases the readout signal. However, the readout signal is ultimately limited by the breakdown of the dispersive limit $n_{\rm crit} = \Delta^2/4g^2 = 500$, above which relaxation increases dramatically. Additionally, the drive power must be below the saturation power of the SLUG. The optimal readout power is $\bar{n} \approx 24$ photons in the cavity and the optimal frequency is $\omega_{\rm read} = 8.0762$ GHz. With these readout parameters, the combined preparation and readout fidelity is 91.9% with $\tau = 200$ ns integration time.

From the histogram (figure 4), we can define the SNR $= |\mu_{\rm g} - \mu_{\rm e}|/(\sigma_{\rm g} + \sigma_{\rm e}) = 3.3$, where $\mu_{\rm g}\,(\mu_{\rm e})$ and $\sigma_{\rm g}\,(\sigma_{\rm e})$ are the means and standard deviations of the distribution of the ground(excited) state. This would correspond to a fidelity of about erf $({\rm SNR}/\sqrt{2}) = 99.9\%$ if SNR were the only cause of fidelity loss, though clearly this cannot be achieved with imperfect preparation and lossy qubits. We can compare this extracted SNR with the theoretical value for resolving two coherent states of the same amplitude with a phase difference 2θ, ${\rm SNR}_{\rm theo} \approx \sin\theta\sqrt{\bar{n}\kappa\tau/(n_{\rm noise} + 1/2)}$. This corresponds to $n_{\rm noise} = 3.2$, which agrees reasonably well with the estimate $k_B T_{\rm noise}/\hbar\omega_{\rm c} \approx$ 2.6–3.6 expected from the observed improvement in noise temperature due to the SLUG and the HEMT device temperature. In fact, the insertion loss of two isolators between the qubit and the SLUG will always make the extracted noise photon higher than that of the amplifier chain. But compared to the HEMT amplifier, the improvement in the SNR allows the observation of quantum jumps in the qubit state [14], and this signal could be used for real-time feedback control [15].

Once the optimal power and frequency have been found for the square pulse, we vary the pulse shape to seek further improvement in readout fidelity. It has been shown [17] that higher fidelity may be achieved with an optimal nonlinear filter rather than with a boxcar filter. Moreover, to achieve fast readout, a sharp initial transient in the pulse is preferable and yet the modulated pulse should not change the qubit state. However, the design of the optimal pulse is not well addressed and proves a difficult problem. In this manuscript, we dynamically search for an optimal pulse using the genetic algorithm. Ideally the algorithm will find the best pulse given the constraint of 200 ns wide boxbar filter while causing mininum change in the state of the qubit.

Specifically, the first 200 ns of the measurement pulse is defined by 20 amplitudes which are polynomially interpolated. A generation in the genetic algorithm is composed of a set of pulses each with randomly generated sets of 20 amplitudes. The pulses that lead to the highest fidelities are then 'bred' together to form a new generation with characteristics that mostly resemble their parent generation. Mutations are added to avoid local extrema. In fact, common pulses are also mixed into the initial generation to speed up convergence. This optimization technique turns out to work well on most of our devices, especially with devices where the intrinsic SNR is not high. Figure 2 shows the results for another sample where the intrinsic SNR is lower than the value reported elsewhere in the paper. The optimal individual pulse converges to the shape with a sharp rising edge, which confirms our speculation that the initial transient of a pulsed measument contains significant amount of qubit-state information. In fact, this pulse shape is in qualitative agreement with the protocol [16] that the experimentally optimal filter should be proportional to the difference between time-dependent ground state and excited state

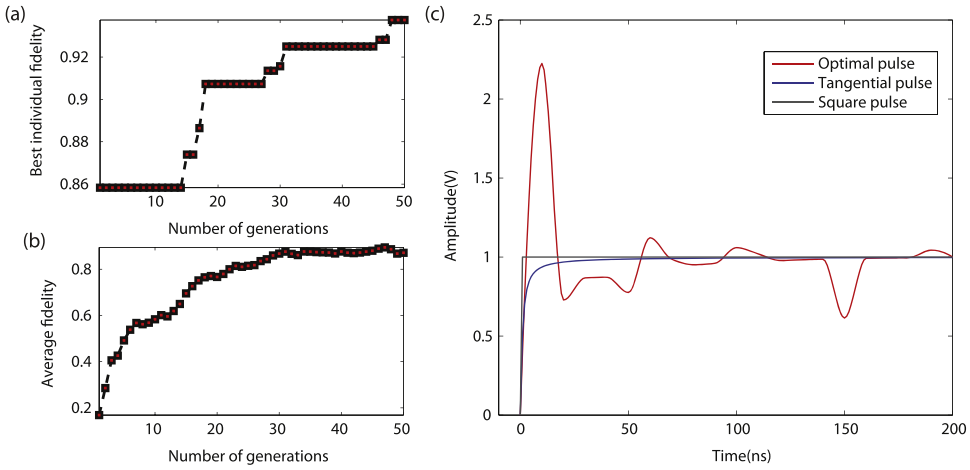

Figure 2. Results of the genetic algorithm. (a) Evolution of best individual fidelity versus generation. (b) Evolution of average fidelity versus generation. (c) The genetic algorithm converges to a family of pulses which highly resemble the optimal pulse shown here. Pulses with tangential rise and square rise are also shown for reference.

responses. The resultant optimal fidelity (92.0%) is higher than the readout fidelity (89.0%) using other common pulses. Genetic algorithm was also applied to optimize the readout pulse for the sample reported in the paper, though here, a family of pulses including the employed square pulse gave approximately the same fidelity. In fact, using the square pulse, other filtering protocols such as an exponentially decaying filter also give the same fidelity [17]. This most likely occurred because of fidelity limitations from other sources such as heating. We believe that this optimization technique can be useful in more complicated cQED architecture where broadband and multitone measurement is necessary.

4. QND measurement, post-selection and randomized benchmarking

This qubit measurement is QND, demonstrated following the techniques of [18]. We apply two consecutive measurement pulses after a $\pi/2$ qubit initialization pulse. Then, we calculate the correlation between the two readout results to determine how measurement affects the qubit state. In a QND measurement with no T_1 processes, these two measurements will be perfectly correlated. A delay between the two pulses are varied to see the time evolution of the correlation. We define the conditional probability $P_{\mathrm{e|e}}(\tau)(P_{\mathrm{g|g}}(\tau))$ that the qubit state is unchanged after the first measurement. We find a very high ground state correlation $P_{\mathrm{g|g}}(\tau = 0) \approx 98.3\%$ (figure 3). The excited state correlation is slightly lower $P_{\mathrm{e|e}}(\tau = 0) \approx 91.1\%$, potentially due to relaxation during the first measurement pulse. We define the full QND fidelity as $F_{\mathrm{QND}} = (P_{\mathrm{g|g}} + P_{\mathrm{e|e}})/2$, yielding $F_{\mathrm{QND}} = 94.7\%$. Considering the heating of the system (see next paragraph), the effective QND fidelity is even higher.

The readout fidelity measured here is a combined preparation and measurement fidelity, as either a preparation or measurement error will lead to a mismatch when comparing expected and measured results. A major source of preparation error is thermal population of the qubit, which is often hotter than the base temperature of the dilution refrigerator [19, 20]. To improve this source of preparation error, active reset methods have been proposed and realized [15, 21].

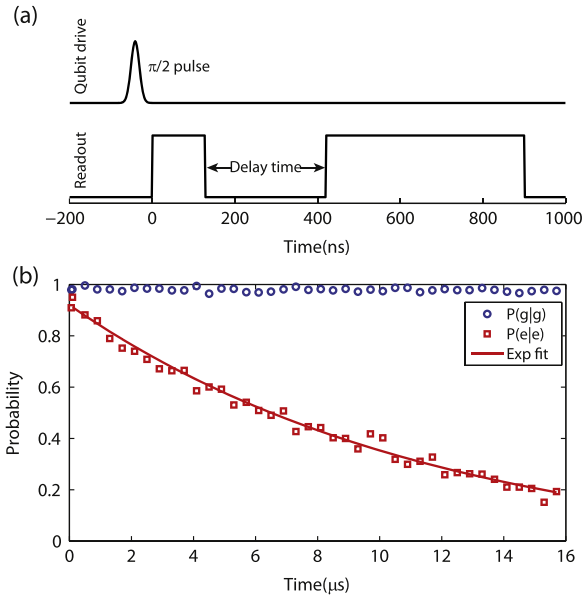

Figure 3. Two pulse correlation measurement. (a) Sequence of qubit control and readout pulses used to determine the dependence of conditional probability on the delay time between two measurements. (b) Time evolution of conditional probability $P_{g|g}(\tau)$ and $P_{e|e}(\tau)$ with an exponential fit. $P_{g|g}(\tau = 0) \approx 98.3\%$, $P_{e|e}(\tau = 0) \approx 91.1\%$.

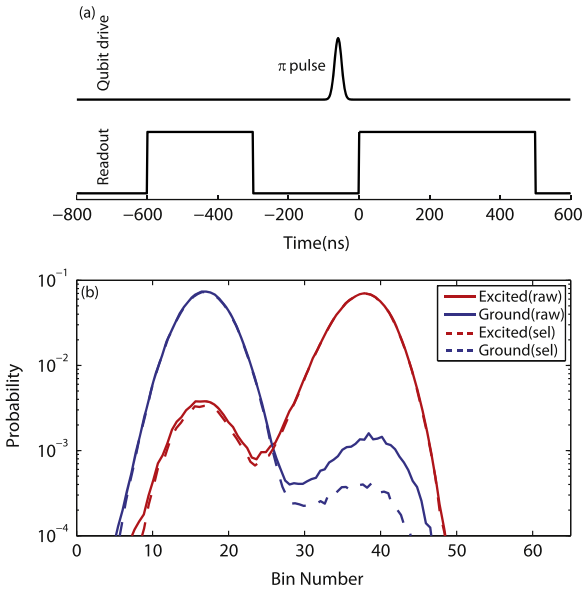

Figure 4. Post-selection measurement. (a) Sequence of qubit control and readout pulses used to suppress errors due to thermal population. (b) Log-linear raw histogram for 400 000 excited and ground state readout events compared with the histogram generated after post-selection. Post-selection is based on the readout result of the first measurement pulse. By eliminating bad preparations in this way, readout error of the excited state decreases from 5.3% to 4.7%, and the ground state from 2.8% to 1.0%. Thus the overall fidelity increases from 91.9% to 94.3%.

In our case, the QND character of the measurement and the small overlap of state distributions make it possible to post-select true ground states before the state preparation [1, 2]. Prior to qubit manipulation, we insert a 320 ns measurement pulse, then wait 300 ns for the cavity to deplete of photons. The events where the qubit is initially determined to be in the excited state are discarded. With this technique and the same 200 ns integration time, the fidelity rises by 2.4%–94.3%. We plot the histogram in log-linear mode and we can see that heating related error is greatly suppressed (figure 4).

After this post-selection technique, there is very little residual preparation error. We use the randomized benchmarking (RB) protocol [22] to quantify this preparation error when preparing the excited state. This RB protocol provides a reliable way to estimate the average error for a set of computational gates by applying a sequence of random gates and examining error accumulation. In this way, the average error of a π pulse is estimated to be 0.5%, which introduces a slight preparation error for excited state preparation. The remaining infidelity is primarily a measurement error due to relaxation during the measurement pulse.

5. Conclusion

To conclude, we have implemented dispersive readout of a transmon qubit with high single-shot fidelity. A low noise SLUG amplifier and other optimization techniques are shown to significantly improve the readout SNR, providing 94.3% combined readout and preparation fidelity with a highly QND measurement. In addition, dynamical optimization of the readout pulse using a genetic algorithm is demonstrated for our system. For our primary sample reported above, the optimal pulse gives same readout fidelity as other common pulses. A similar result is recently reported [23]. As the SLUG requires only dc bias, has high dynamic range, and can easily be isolated from the qubit, it provides a possible alternative to parametric amplifiers. Fidelities larger than 98% could be possible in devices with $T_1 > 10\ \mu$s [24–26].

Acknowledgement

This work was supported by IARPA under Contract W911NF-10-1-0324

References

[1] Johnson J E *et al* 2012 *Phys. Rev. Lett.* **109** 050506
[2] Ristè D *et al* 2012 *Phys. Rev. Lett.* **109** 050507
[3] Hatridge M *et al* 2013 *Science* **339** 178
[4] Johnson J E *et al* 2011 *Phys. Rev.* B **84** 220503(R)
[5] Hoffman A J *et al* 2011 *Phys. Rev. Lett.* **107** 053602
[6] Spietz L *et al* 2008 *Appl. Phys. Lett.* **93** 082506
[7] DeFeo M P *et al* 2010 *Appl. Phys. Lett.* **97** 092507
[8] DeFeo M P and Plourde B L T 2012 *Appl. Phys. Lett.* **101** 052603
[9] Ribeill G J *et al* 2011 *J. Appl. Phys.* **110** 103901
[10] Hover D *et al* 2012 *Appl. Phys. Lett.* **100** 063503
[11] Abdo B *et al* 2014 *Phys. Rev. Lett.* **112** 167701
[12] Schuster D I *et al* 2005 *Phys. Rev. Lett.* **94** 123602
[13] Reed M D *et al* 2010 *Phys. Rev. Lett.* **105** 173601

[14] Vijay R *et al* 2011 *Phys. Rev. Lett.* **106** 110502
[15] Ristè D *et al* 2012 *Phys. Rev. Lett.* **109** 240502
[16] Ryan C A *et al* 2013 arXiv:1310.6448
[17] Gambetta J *et al* 2007 *Phys. Rev.* A **76** 012325
[18] Lupaşcu A *et al* 2007 *Nat. Phys.* **3** 119
[19] Córcoles A D *et al* 2011 *Appl. Phys. Lett.* **99** 181906
[20] Barends R *et al* 2011 *Appl. Phys. Lett.* **99** 113507
[21] Geerlings K *et al* 2013 *Phys. Rev. Lett.* **110** 120501
[22] Magesan E *et al* 2011 *Phys. Rev. Lett.* **106** 180504
[23] Hover D *et al* 2014 *Appl. Phys. Lett.* **104** 152601
[24] Chang J *et al* 2013 *Appl. Phys. Lett.* **103** 012602
[25] Paik H *et al* 2011 *Phys. Rev. Lett.* **107** 240501
[26] Rigetti C *et al* 2012 *Phys. Rev.* B **86** 100506(R)